Fermi National Accelerator Laboratory

FERMILAB-Pub-91/115

A Trigger for the Fermilab E760 Lead-Glass Calorimeter

R. Ray, J. L. Rosen, M. Masuzawa, J. Zhao
Fermi National Accelerator Laboratory
P.O. Box 500
Batavia, Illinois 60510

May 1991

* To be submitted to *Nuclear Instruments and Methods A*

A Trigger for the Fermilab E760 Lead-Glass Calorimeter

R. Ray* J. L. Rosen M. Masuzawa
J. Zhao
Northwestern University, Evanston, IL 60208

Abstract

The E760[1] experiment at Fermi National Laboratory has been commissioned to study electromagnetic decay channels of charmonium states. A trigger has been built for the 1280-element lead-glass calorimeter to facilitate the study of all-neutral decay modes. The trigger has also proven to be extremely useful for charged electromagnetic final states. The trigger has been successfully deployed and has shown itself to be reliable and highly efficient. The design and performance of this trigger are described in detail.

1. Introduction

Fermilab experiment 760 is a charmonium formation experiment designed to study the electromagnetic decays of resonantly produced states from $\bar{p}p$ annihilations in order to accurately measure their masses, widths, branching ratios and angular distributions. The E760 detector efficiently detects electromagnetic decays of charmonium states while at the same time rejecting large non-resonant hadronic background. Many of these resonances decay to all-neutral final states containing two or more gamma rays possessing a GeV or more of lab energy ($\eta_c \rightarrow \gamma\gamma$, for example). In order to trigger on such all-neutral states, signals from the E760 lead-glass calorimeter must be processed. The calorimeter is also useful as part of a charged particle trigger for decay channels such as $\psi \rightarrow e^+e^-$ and $\chi_{1,2} \rightarrow e^+e^-\gamma$. This paper describes the trigger which has been built for the E760 calorimeter. The performance of the trigger during the experiment's first physics run is also discussed.

The E760 detector is shown in figure 1. It consists of scintillation hodoscopes and vetos, tracking chambers [1], a segmented threshold Cerenkov counter, a forward sampling electromagnetic calorimeter [2] and a central electromagnetic calorimeter [3]. The central calorimeter consists of 1280 lead-glass blocks, each of which points directly back to the interaction vertex formed by the $\bar{p}$ beam and a hydrogen gas-jet target. Two of the calorimeter "wedges" are shown in figure 1. A wedge contains

*Presently at Fermi National Laboratory, Batavia, IL 60510

[1]Fermilab, Ferrara, Genova, U.C. Irvine, Northwestern, Penn. State, Torino collaboration

20 blocks, each of different size, and fills the polar-angle range of 10° to 70°. There are 64 identical wedges which fill the full azimuthal range of 360°. Each set of 64 identical blocks sharing the same polar-angle constitutes a "ring."

The unique geometry of the calorimeter is such that the transverse dimension of the blocks decreases as the polar angle decreases. The photomultiplier tubes which are attached to each block also correspondingly decrease in size. Four different sizes of tubes are used (3″, 2.5″, 2″ and 1.5″) and each size has its own pulse shape characteristics. The need to accommodate these different pulse shapes was a significant consideration in the design of the calorimeter trigger.

The charged trigger can easily be reduced to manageable levels by invoking a Cerenkov requirement to identify electrons; however, no such mechanism is available for all-neutral decays. The total $\bar{p}p$ cross section in the charmonium region is about 70 mb. This translates into a 700 kHz interaction rate for the maximum luminosity expected by the experiment of $10^{31} cm^{-2} s^{-1}$. The total annihilation cross section at a center-of-mass energy of 3.550 GeV is 22 mb[5]. The all-neutral cross-section is 1-2% of the annihilation cross section[6], resulting in an all-neutral trigger rate of 4.4 kHz. The calorimeter trigger must reduce this rate to less than 1 kHz to avoid excessive deadtime in the CAMAC readout. Monte Carlo studies indicate that a simple transverse momentum cut of 0.6 GeV/c should reduce the all-neutral trigger rate to 1.4 kHz. Requiring two clusters with large transverse momentum should reduce the rate to 360 Hz. The errors on these numbers may be quite large due to the uncertainty with which one knows the relative cross sections of the various $n\pi^o$ channels. However, it is clear that the rate of the all-neutral trigger may be reduced to quite acceptable levels with a minimum of hardware bias.

The basic philosophy of the trigger is to reduce the number of elements in the decision-making process from 1280 (the number of calorimeter cells) to a more manageable number while at the same time requiring at least two significant deposits of transverse electromagnetic energy. This is accomplished by analog summing of the signals from adjacent calorimeter modules into 40 "super-clusters." Due to the transverse spread of electromagnetic showers, significant deposits of energy in the calorimeter will often span super-cluster boundaries. In order to form a fully efficient trigger one must compensate for this by setting appropriately low thresholds, or by forming sums which include overlaps sufficient to contain most of the energy in a single super-cluster. The latter option has been chosen because of the adverse effect that lowered thresholds would have on the trigger rate.

The 40 signals which result from the summing procedure are subjected to an energy threshold by a set of discriminators. The logic outputs from the discriminators then undergo some simple pattern recognition. A schematic of the calorimeter trigger is shown in figure 2. The level I summer, level II summer, integrator module and OR module are the subject of this paper and will be described in detail.

2. Level I Summer

The level I summers are located in the E760 experimental area and are mounted in racks directly adjacent to the calorimeter. Each 19″ x 10.5″ x 3″ unit is divided into identical halves, each half handling the signals from a single ring of 64 identical lead-glass blocks. There are 10 such units in all which process the signals from all 20

rings. A circuit diagram appears in figure 3.

Each input signal to the front of the summer comes directly from the output of the photomultiplier tube connected to a single glass block. 95% of this signal is split off by a simple resistor network and is sent back out of the summer on a connector which is adjacent to the input connector. This feedthrough signal is then propagated along delay cables to an ADC channel. The remaining 5% of the charge is summed with 5% of the signals from adjacent calorimeter modules within the same ring, into the virtual ground node formed at the inverting input of an op amp. The summing pattern around each ring is shown in table 1. Eight sums are formed from regions within each ring known as "super-wedges" for a total of 160 level I trigger sums. Each of the sums shares an overlap with each of its two adjacent sums. The overlap is accomplished by a split through a pair of 2490 Ω resistors, with half of the signal being sent to each of the two sums. The signals which do not participate in an overlap are treated similarly. Half of the signal is sent to the appropriate sum through a 2490 Ω resistor while the second half is drained to ground through a 2490 Ω load resistor. This assures uniform response for all input channels.

Once the sums have been formed, they are amplified (x10) in an inverting amplifier circuit using a Comlinear CLC401AJP wideband, fast-settling op amp. The CLC410AJP is a high-gain monolithic op amp which employs a unique current feedback topology. It has a -3 db bandwidth of 150 MHz, a rise/fall time of 2.5 ns and a slew rate of 1200 V/μs. The power dissipation of the chip is 150 mW. The 160 amplified sums, available at the rear of each unit, are 50 Ω back terminated and AC coupled.

The level I summing scheme is in effect, incorporated into a large convenient patch-panel. The inputs are arranged in a wrap-around configuration which was developed to minimize the space separating the relevant inputs from the relevant summing amplifier. Internal coaxial cables and a large number of buffer stages have been avoided. The front panel layout of the level I summer is shown in figure 4. Note that input 1 is adjacent to input 64. The feedthrough outputs are face-centered on the input matrix. The input connector spacing is 1". The high density of connectors is accommodated during cabling with the aid of a commercially available cable gripping tool.

3. Level II Summer

The level II summers are double-width NIM modules which reside in the E760 counting room directly above the E760 detector. There are eight such units, each of which processes the 20 signals (1 per ring) from one of the 8 super-wedges formed by the level I summers. Each of the 20 input signals, which enter the module from the back, are split by a resistor network which sends 5% of the signal to a summing junction and the remainder to an inverting feedthrough circuit. A circuit diagram appears in figure 5.

The summing circuit for the level II summer is similar to that of the level I summer. Each module forms 5 overlapping sums by adding signals from adjacent rings within the same super-wedge according to the pattern described in table 2. The 5 groups of rings are known as "super-rings." In the case of the level I summers, the signals are summed through 2490 Ω resistors. In this case the 20 signals are weighted

by the summing resistors in such a way as to equalize the expected energy deposit within the angular range of a super-ring, based on two-body kinematics. The weighting allows for a cleaner threshold determination. This is demonstrated in figure 7 where a Monte Carlo has been used to generate the decay kinematics for $\psi \rightarrow e^+e^-$. The weighting factors and resistor values are shown in table 3. One set of weighting resistors works for the entire range of the experiment. The signals which participate in overlaps are weighted differently for each of the two sums to which they contribute. In order to maintain a constant input impedance for each channel the value of the load resistors are adjusted in order to give an equivalent resistance of 1245 Ω when combined in parallel with the weighting resistors. The weighting and load resistors are of the metal film variety and have a tolerance of 1%.

Once the signals have been weighted and summed the inverting amplifier restores the sums to negative polarity while amplifying them by a factor of 10. The outputs are series terminated into 50 Ω and AC coupled through a 0.1 mF capacitor. This results in 40 super-clusters which contain all of the energy deposited in the calorimeter. The super-clusters are configured in a 5 super-ring by 8 super-wedge array and each super-cluster has a 1 block overlap at all interior boundaries. The super-cluster structure is illustrated in figure 6 by a beams-eye-view of the calorimeter. Two of the 40 super-clusters are highlighted by cross-hatching. The dashed lines indicate the overlap boundries.

The super-cluster sums are fanned out 4 times within the module by emitter-follower transistor networks. One of the four outputs is sent to the next module in the trigger chain containing an integration circuit, described below, and then on to the energy discriminators. A second output is sent to an ADC channel. This digitized signal is used to monitor the performance of the trigger and the settings of the energy thresholds. A third output is sent to another ADC channel, but its arrival is delayed by 100 ns relative to the signal at the former ADC. This serves as a pre-trigger snapshot indicating the presence of tails from previous interactions imbedded in a particular event. The last of the 4 fanned-out signals is available for some future contingency.

The inverting feedthrough circuit is a transistor network which receives 95% of the signal from each of the 20 inputs to the level II summer. The circuit independently re-inverts and amplifies each of the 20 inputs by a factor of 1.5. These signals are sent to a set of "minimum-bias" discriminators (LeCroy 4413) whose thresholds are set as low as possible (about 17 mV). The low thresholds are intended to minimize time-jitter on the discriminator outputs. The output from the minimum-bias discriminators determines the timing for the experiment.

4. Integrator Module

Circuits designed to handle photomultiplier pulses at the trigger level are typically of the peak sensing type. However, the total charge contained within the pulse is the more relevant quantity since it is this charge which is proportional to the energy deposited in a detector and recorded using a charge-sensitive ADC. In addition, the total charge experiences smaller fluctuations than the pulse amplitude. The total charge is also independent of pulse shape, an important consideration in this case because of the sums formed by contributions from different sizes of photomultiplier

tubes. For all of these reasons, an integration circuit has been developed to process the signals from the level II summers. The integration circuits are housed in single-width NIM modules, 16 channels per module. The input current is clipped with a shorted cable connected to the rear of the module which produces a bipolar signal. The clip time is $2t = 32$ ns. The bipolar signal is integrated with a time constant of 500 ns. A circuit diagram appears in figure 8. Clipping before integration reduces the possibility of pile-up in the integration capacitor and results in a simpler circuit. In spite of the long integration time constant, the clipping cable brings the output from the integrator back to its baseline in about 100 ns. The amplitude of the output pulse is proportional to the total charge contained in the input pulse. The integrator circuit converts input charge to an output voltage at the rate of about 2 mV per pC.

It should be noted that the total charge signal is slower than the unintegrated signal. Accurate charge determination requires that one wait until most of the charge has been deposited. The total charge signals will also experience more time slewing in the energy discriminators. This is of little consequence since the trigger is eventually re-clocked with the minimum-bias signals.

5. Energy Discriminators and OR Module

Once the 40 super-clusters have been integrated, they are sent to one of five LeCroy 4413 CAMAC discriminator modules. The 4413 is a 16-channel discriminator unit with ECL level outputs and a remotely programmable threshold common to all 16 channels. The 8 signals from each super-ring are sent to the same discriminator module and thus subjected to the same threshold. The remaining 8 channels of the discriminator module are unused. The thresholds are determined from simple kinematics and increase with each successive super-ring.

The digital ECL level outputs from the energy discriminators are passed on to the OR module. The OR module consists of eight 5-input OR circuits (Signetics 100101 triple 5-input OR chips) housed in a double-width NIM module. The module internally routes the signals from the 5 super-rings in a given super-wedge to a single OR chip. The 8 ECL level outputs from the OR module represent the energy deposition above threshold in each azimuthal octant of the calorimeter. The octants retain the overlap structure at super-wedge boundaries built into the wedge-summing scheme at the level I summers.

A 16-bit memory lookup unit (MLU) [4] is used to perform pattern recognition on the 8-bit word which results from the OR module. For 2-body decays such as $\psi \rightarrow e^+e^-$ the MLU looks for back-to-back octants with energy deposition above threshold by requiring, for example, that bits 1 and 5 be simultaneously set. For 3-body decays, such as $\chi_{1,2} \rightarrow \psi\gamma \rightarrow e^+e^-\gamma$ where the ψ decay is slightly Doppler-broadened, the MLU relaxes its back-to-back requirement somewhat by searching for one octant in coincidence with one of the opposite 3 octants. The logic loaded into the MLU is inclusive, allowing for bits to be set other than those which are required. This is necessitated by the overlaps.

The MLU module is strobed by the gate generated by the minimum-bias discriminators. Any signals present on the input lines when the module is strobed are loaded into the input register. The module searches its memory to see if the inputs match one of the down-loaded combinations which correspond to a valid trigger. If a

valid combination exists a NIM level output is generated. The MLU output is sent to a second MLU where it is combined with trigger information from other detector elements before a final decision is made. An all-neutral trigger, for instance, would require a signal from the first MLU, and would allow no hodoscope elements to be present in the second MLU.

6. Performance of the Trigger and its Components

The calorimeter trigger has been used during the 1990 run of the E760 experiment. Additionally, the level I summers were used during calorimeter calibration runs performed in an electron beam at Brookhaven National Laboratory in 1989 [3]. During the running at Brookhaven, the linearity of the level I summer was checked by exposing three lead-glass wedges to a 3 GeV/c electron beam. The hardware sums were digitized and compared off-line to the reconstructed software sums. The results of the comparison are shown in figure 9 where the software sum is plotted against the hardware sum (a). The percentage residuals are also shown (b). The upper band in figure 9a corresponds to direct hits in the central wedge while the lower band corresponds to leakage into the two adjacent wedges. The slope of the distribution in figure 9a is 0.505, consistent with attenuation by a factor of 2 (2.08) at the level I summer and the fact that only 95% of the signal from the lead-glass modules is passed to the ADC's. The width (σ) of the residual distribution in figure 9b is 0.4%.

The combined performance of the level I and level II summers has been checked with data from the 1990 E760 run. The hardware sums from the level II summers are digitized during normal data taking as a diagnostic on the trigger. The results of the comparison between these hardware sums and the reconstructed software sums are shown in figure 10, which is similar to figure 9. The data were taken while scanning the ψ' resonance. The amplitude of the hardware sums is attenuated by about a factor of 2 at both the level I (2.08) and level II (2.17) summers before being digitized. The signals from the lead-glass blocks from which the software sums are formed are attenuated by a factor of 2 by a card at the face of the ADC module. The slope of the distribution in figure 10a is 0.46, consistent with the attenuation factors. The width of the residuals in figure 10b is 2.4%.

The linearity of the integration circuit has been bench tested by injecting a known amount of charge from a precision capacitor into the circuit. The results are shown in figure 11 where the output voltage is plotted as a function of the input charge. The χ^2/d.o.f. which results from a fit to a straight line is 1.3. The linearity seems to begin falling off for input charges approaching 400 pC, but this is well above the region where thresholds are set. The largest thresholds which might be expected are in the 200 pC range.

The performance of the overall trigger has been tested using data taken at the ψ resonance. Parallel triggers, one of which required a signal from the calorimeter trigger and one which did not, were run simultaneously. The latter trigger required signals to be present in opposite sides of the hodoscopes and the Cerenkov counter, consistent with ψ decay to e^+e^-. The data acquired using this trigger were analyzed for ψ's and the performance of the calorimeter trigger was evaluated for these events. The value of the hardware sum from the level II summers is plotted vs. the ring number struck by the particle in figure 12a for both tracks of these reconstructed

ψ's. When requiring that both the electron and positron be within the calorimeter acceptance at the ψ center-of-mass, the calorimeter is populated only out to ring 13. Additionally, the hodoscope trigger does not cover rings 1 and 2. In figure 12b the hardware sum as a function of ring number is plotted for all sums for which the corresponding pattern unit bit is set. The pattern units are fed by the second outputs of the energy discriminators. The lower edge of the distributions in figure 12b indicates the settings and sharpness of the energy thresholds. Comparing figure 12a with 12b demonstrates that the energy deposition from the e^+e^- tracks resulting from ψ decay are comfortably above the threshold settings. Comparisons between the two parallel triggers show the calorimeter trigger to be better than 99% efficient.

Electron pairs from inclusive decays of the ψ, such as $\chi_{1,2} \rightarrow \psi\gamma \rightarrow e^+e^-\gamma$ and $\psi' \rightarrow \psi\pi\pi \rightarrow e^+e^-\pi\pi$, have been triggered on with equal success. The explicit energy-angle correlation which holds for exclusive ψ decays also holds approximately for inclusive decays since, in the energy range of interest, the relatively massive ψ receives only a modest kick from the recoil particles. This results in an inclusive decay which is only slightly Doppler-broadened and requires no special treatment with respect to super-ring thresholds.

The calorimeter trigger has also been used to trigger on all-neutral final states. Neutral data have been taken in order to determine trigger rates, measure backgrounds, collect π° data for purposes of calibration and to search for the decay $\chi_2 \rightarrow \gamma\gamma$. The all-neutral trigger rate at the ψ resonance is about 50 Hz, normalized to a luminosity of $10^{31} cm^{-2} s^{-1}$. For running at the ψ the MLU is downloaded with a strict back-to-back requirement. The normalized all-neutral rate at the χ_2 resonance is 450 Hz. Because the three-body charged decay mode $\chi_2 \rightarrow \psi\gamma \rightarrow e^+e^-\gamma$ is being triggered on simultaneously, the MLU requirements are relaxed to allow one calorimeter octant to be in coincidence with any one of the opposite 3 octants. This results in a higher neutral trigger rate. These trigger rates produce no deadtime problems.

7. Conclusion

A trigger incorporating the E760 calorimeter as a central component has been designed, built and successfully deployed. The trigger is fully efficient and successfully reduces the large non-resonant hadronic and all-neutral backgrounds to manageable levels. As E760 continues its program of resonant charmonium spectroscopy, the calorimeter trigger will be used to search for all-neutral decay modes of the η_c, η_c', χ_2 and $^1P_1$ states. It will also continue to be a valuable component of the charged particle trigger.

8. Acknowledgments

We would like to thank Robert Tilden of Northwestern University for his skill and expertise during the design and construction of the trigger modules. We would also like to thank our E760 colleagues for their many valuable suggestions and comments. The efforts of the Fermilab staff, and in particular those associated with running the antiproton source, are much appreciated as well. This work has been supported in part by U. S. Department of Energy contract DE-AC02-76ER02289.

References

[1] C. Biino et al., NIM **A271** (1988) 417; C. Biino et al., IEEE Trans. Nucl. Sci. **36** (1989) 98; R. Calabrese et al., IEEE Trans. Nucl. Sci. **36** (1989) 54; R. Calabrese et al., NIM **A277** (1989) 116.

[2] M. A. Hasan et al., NIM **A295** (1990) 73.

[3] L. Bartoszek et al., NIM **A301** (1991) 47.

[4] T. Regan, Fermilab-FN-544, (1990).

[5] K. Böckmann et al., NC **44A** (1966) 316.

[6] C. N. Booth et al., PR **D27** (1983) 2018.

Table 1. The summing pattern for the level I summers around a given ring.

Super-Wedge Number	Wedge Numbers From a Given Ring
1	1-9
2	9-17
3	17-25
4	25-33
5	33-41
6	41-49
7	49-57
8	57-1

Table 2. The summing pattern for the level II summers for a given super-wedge.

Super-Ring Number	Ring Numbers From a Given Super-Wedge
1	1-4
2	4-8
3	8-12
4	12-16
5	16-20

Table 3. Value of the weighting resistors and the relative weights for each input channel of the level II summer. The channels which participate in overlaps have two weighting resistors. The ratios are calculated relative to the central channel in each sum (channels 2, 6, 10, 14 and 18).

Input Channel	Resistor Value (ohms)	Relative Weight
1	2260	1.10
2	2490	1.00
3	2740	0.91
4	3090,2050	0.81,1.21
5	2260	1.10
6	2490	1.00
7	2740	0.91
8	3010,2100	0.83,1.19
9	2320	1.07
10	2490	1.00
11	2610	0.95
12	2740,2260	0.91,1.10
13	2370	1.05
14	2490	1.00
15	2610	0.95
16	2670,2370	0.93,1.05
17	2430	1.02
18	2490	1.00
19	2550	0.98
20	2610	0.95

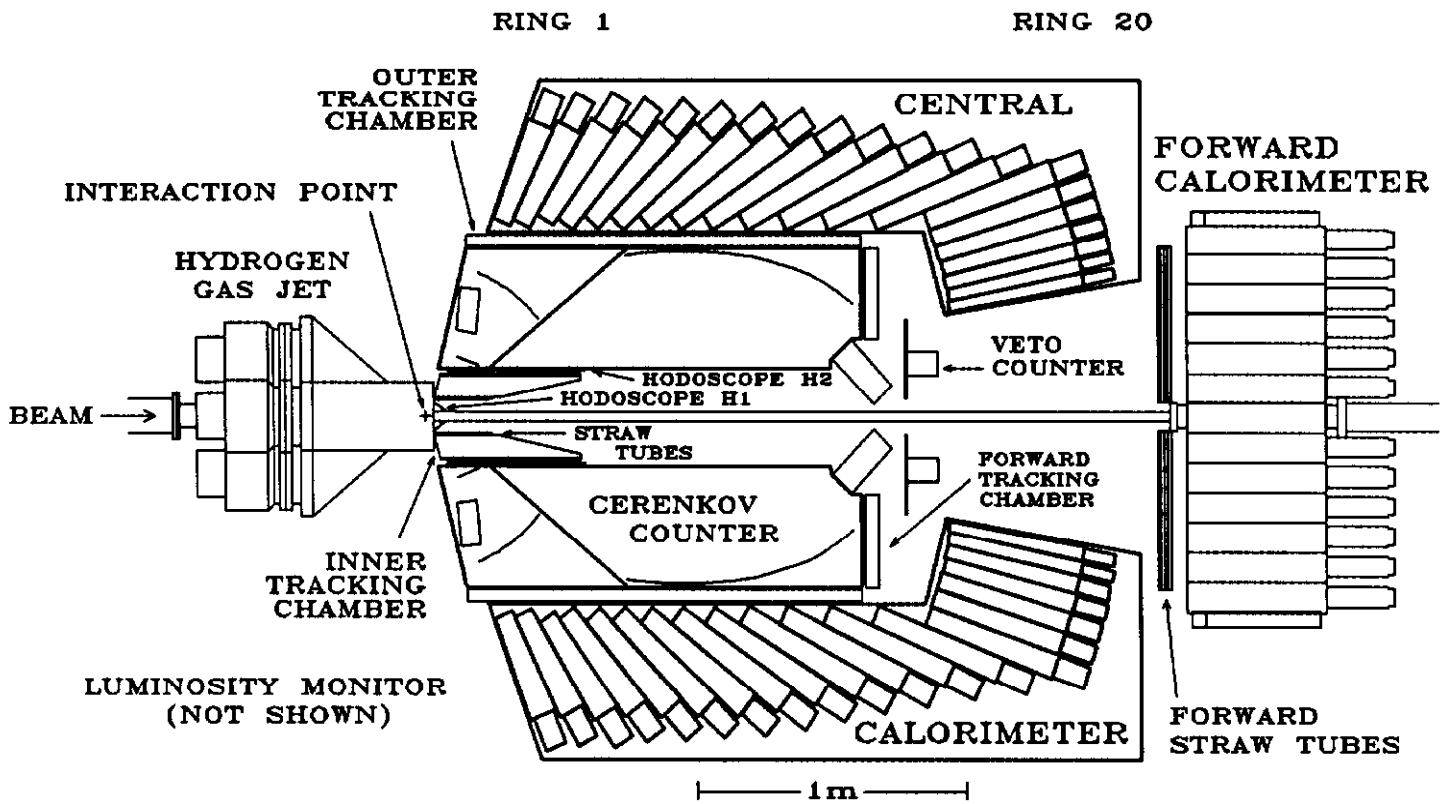

Fig. 1. The E760 detector layout. The 1280-element lead-glass central calorimeter surrounds the tracking chambers and the gas-threshold Cerenkov counters. Two of the 64 calorimeter wedges are shown. Each wedge contains 20 blocks which belong to one of 20 rings. Ring 1 begins at 70° with respect to the beam axis and ring 20 ends at 10°.

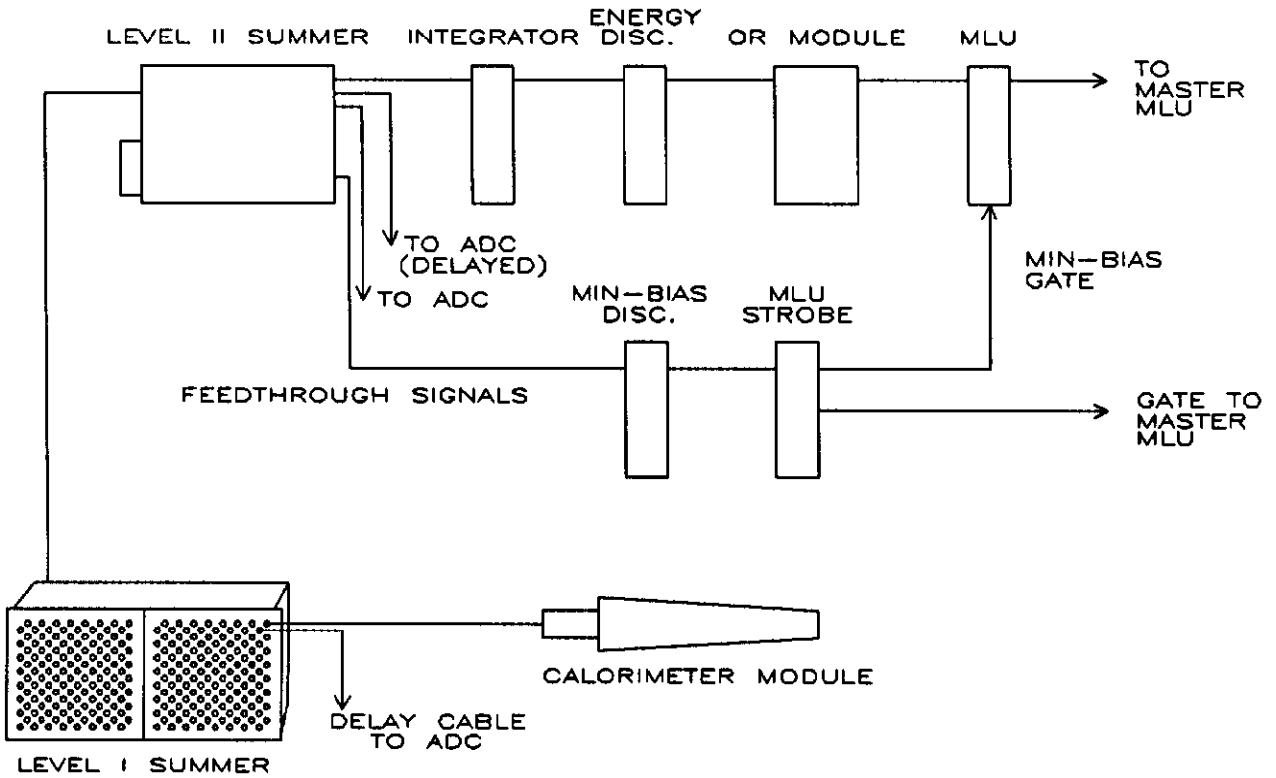

Fig. 2. Schematic of the E760 calorimeter trigger.

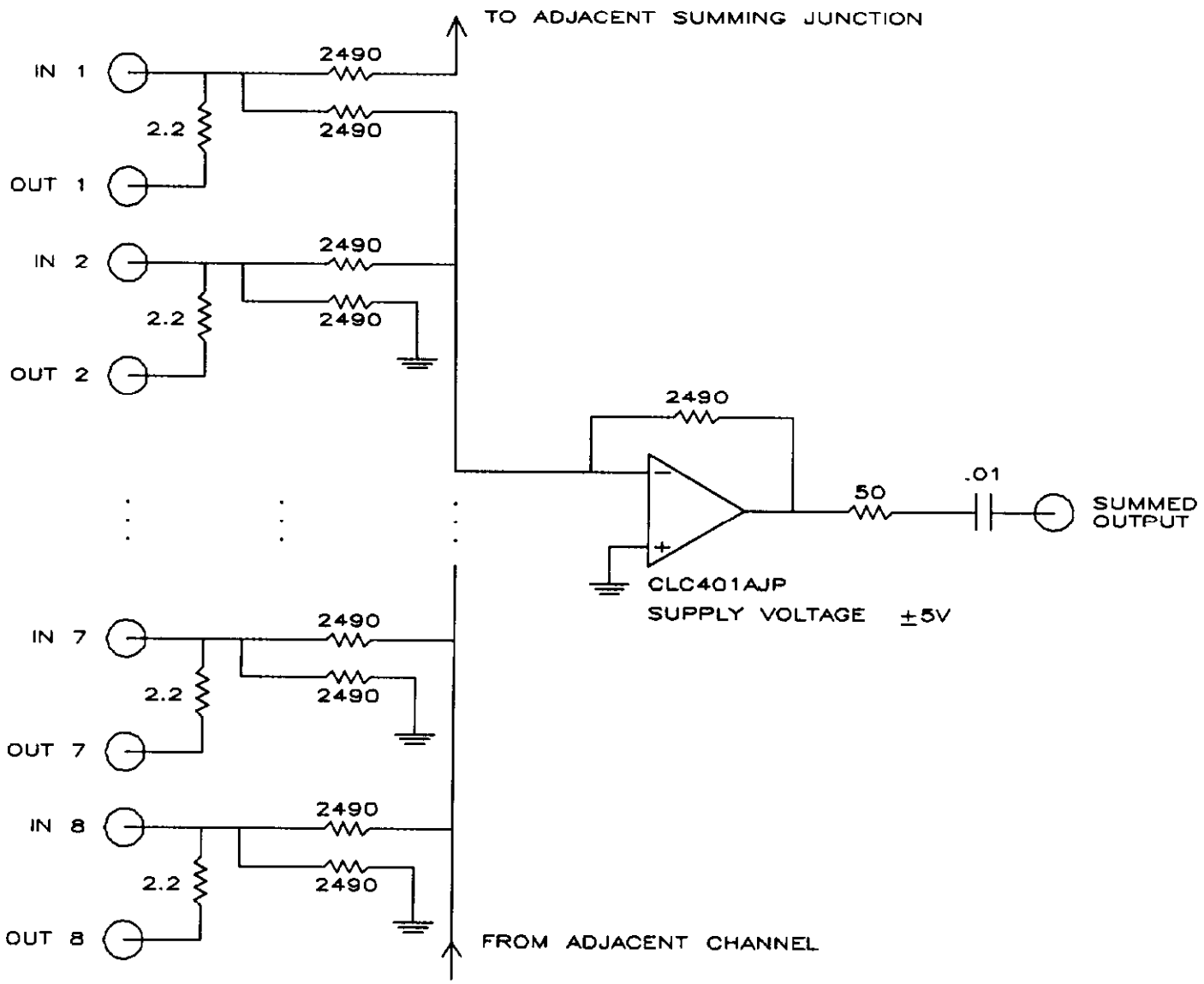

Fig. 3. Circuit diagram for the level I summers. Resistor values are in ohms and capacitor values are in μF.

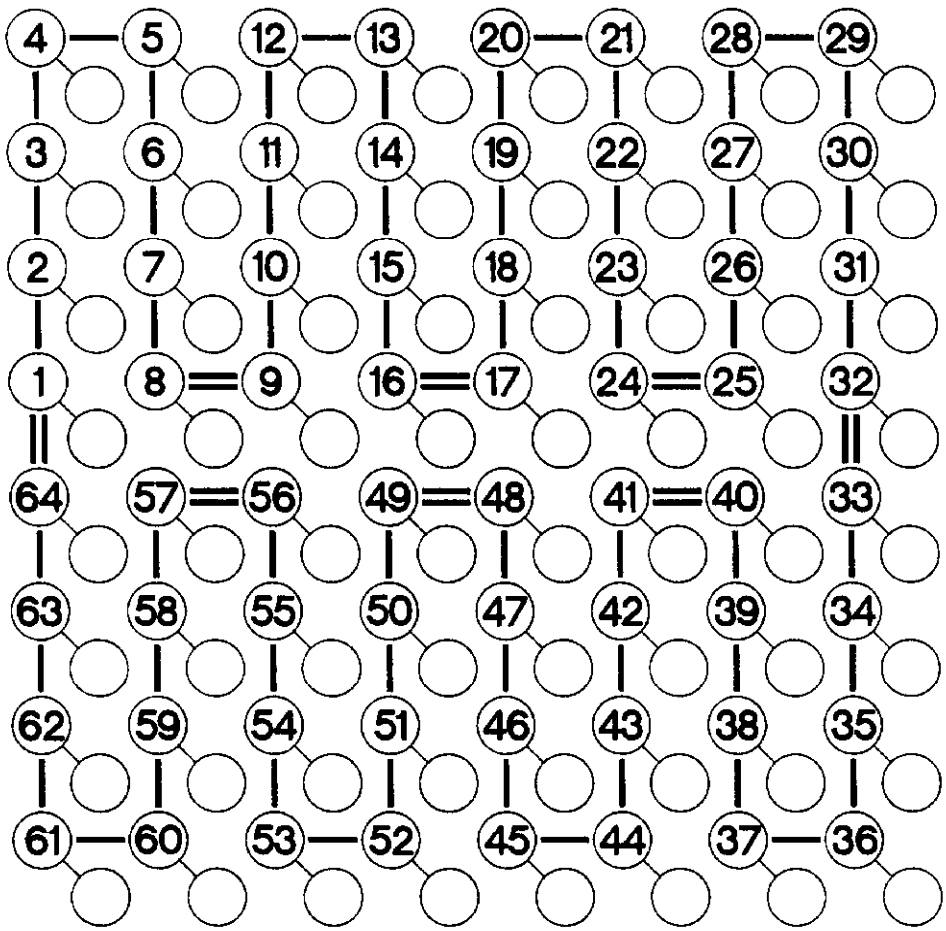

Fig. 4. The front panel layout for the level I summer. The wrap-around layout is such that the relevant input connectors are as close as possible to the relevant summing amplifier. The input connectors are numbered and the feedthrough outputs are face-centered on the input matrix. The spacing between input connectors is 1″.

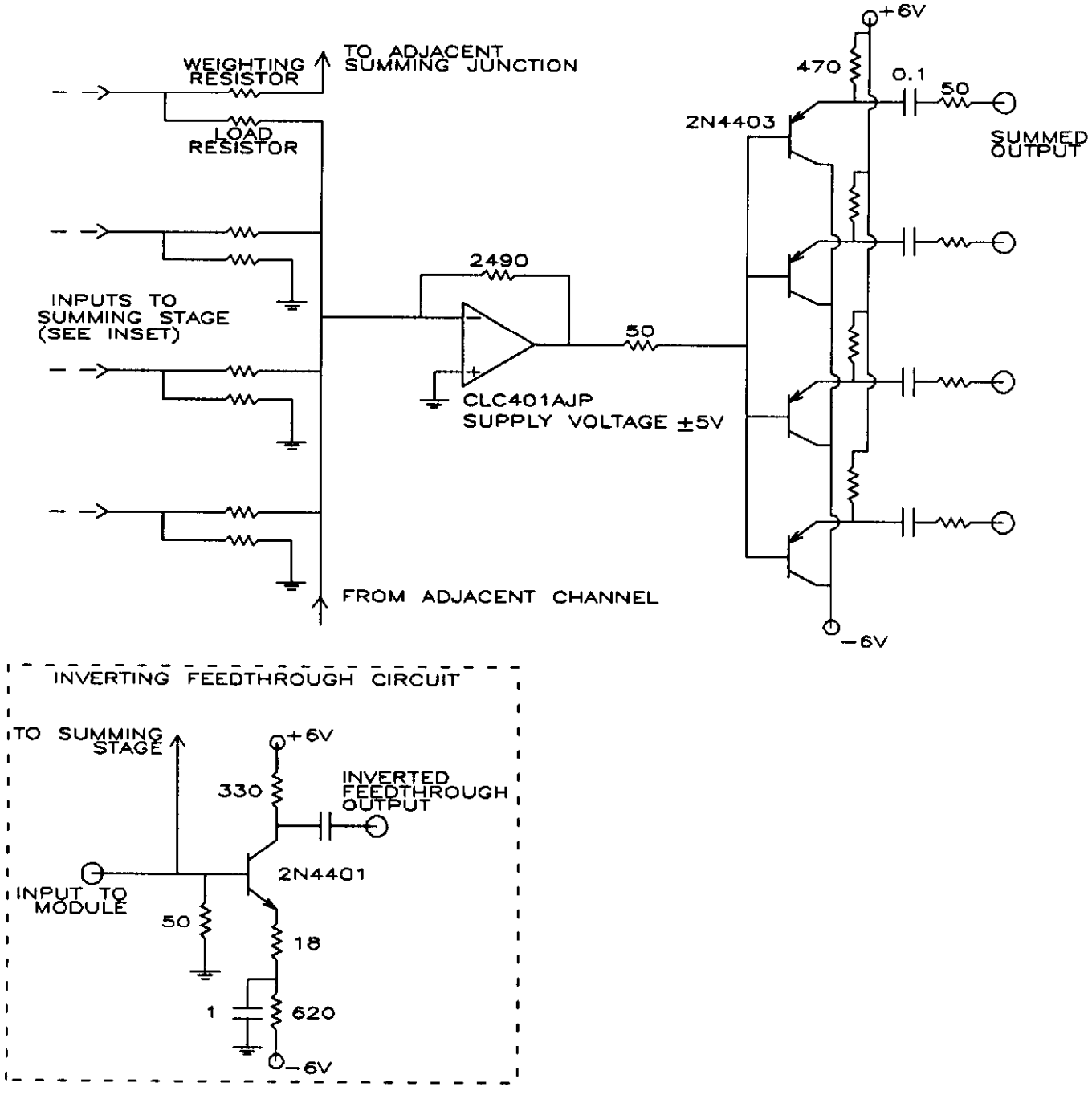

Fig. 5. Circuit diagram for the level II summers. 5% of the input signal is sent to the summing junction and the remainder goes to the inverting feedthrough circuit (see inset). Resistor values are in ohms and capacitor values are in μF.

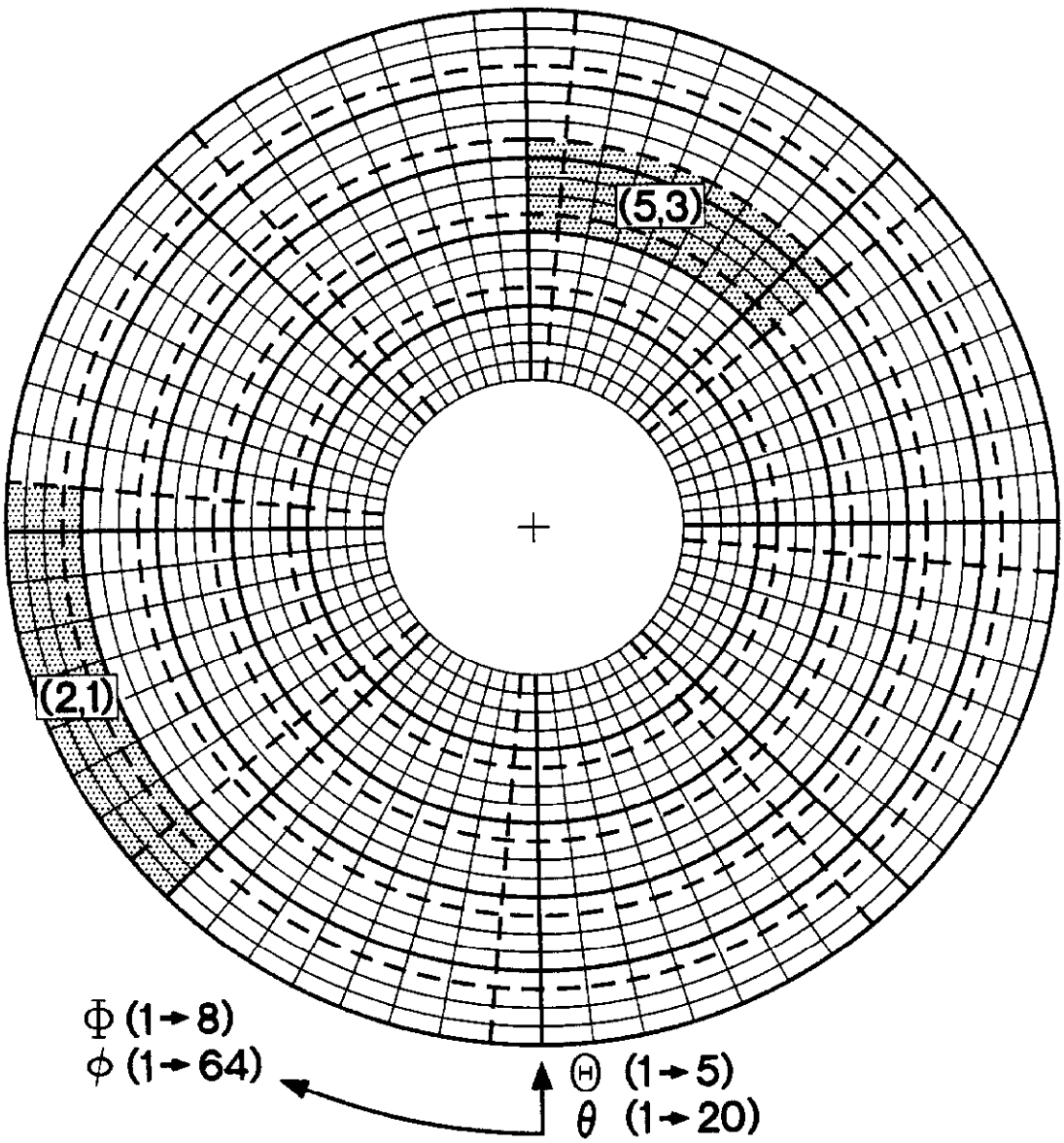

Fig. 6. A beams-eye view of the calorimeter showing the structure of the 40 overlapping super-clusters which are arranged in a 5 (Θ) x 8 (Φ) array. The overlaps are indicated by the dashed lines and are described in tables 1 and 2. $(\Phi, \Theta) = (2,1)$ and (5,3) are crossed-hatched as examples.

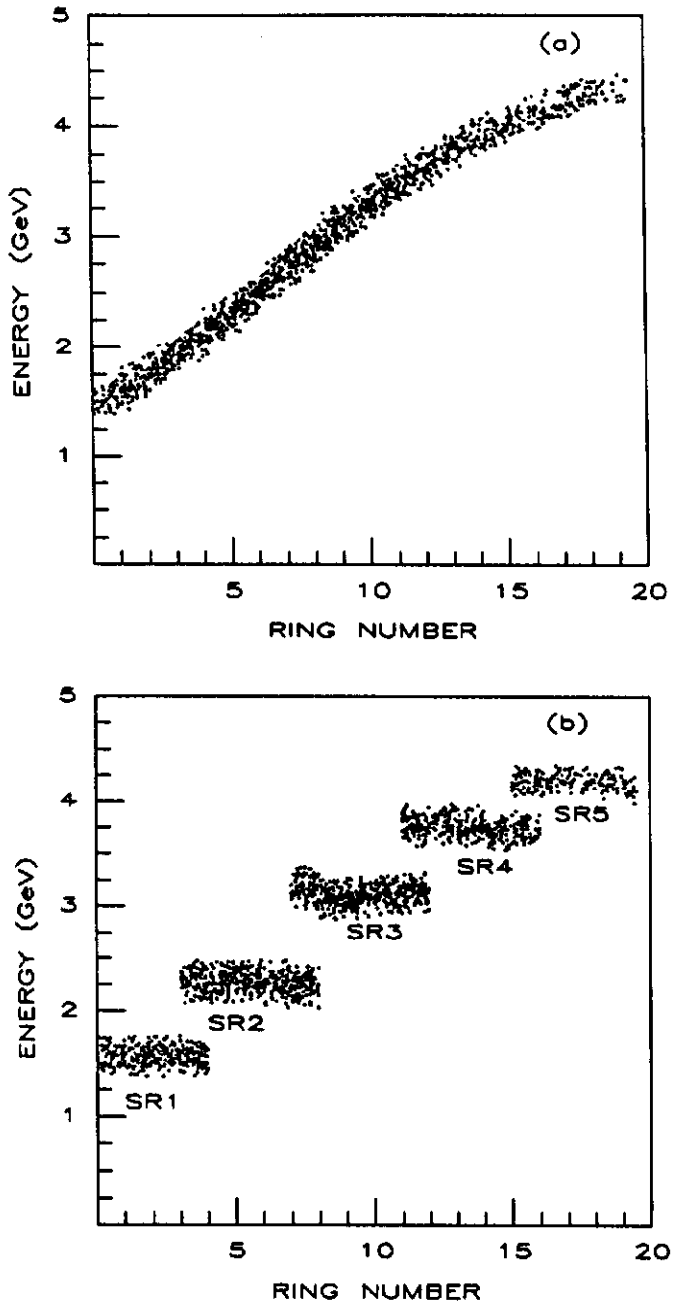

Fig. 7. Monte Carlo simulation of the kinematics for the process $\psi \rightarrow e^+e^-$. The ring number impacted by the electron (positron) is ploted vs. the energy of the particle for the case when the deposited energy is unweighted (a) and when the deposited energy is adjusted according to the weighting scheme of the level II summers (b).

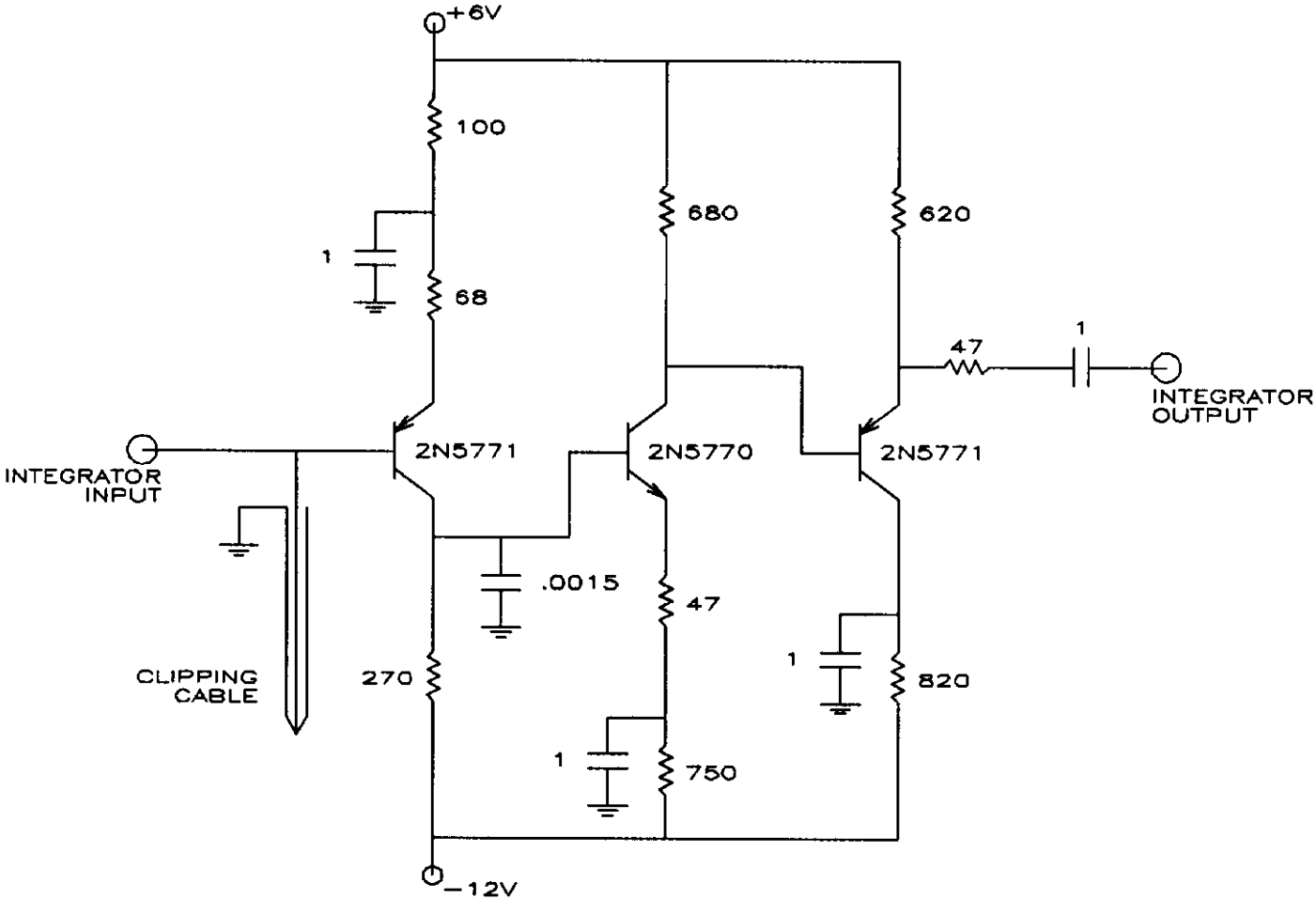

Fig. 8. Circuit diagram for the integrator module. Resistor values are in ohms and capacitor values are in μF.

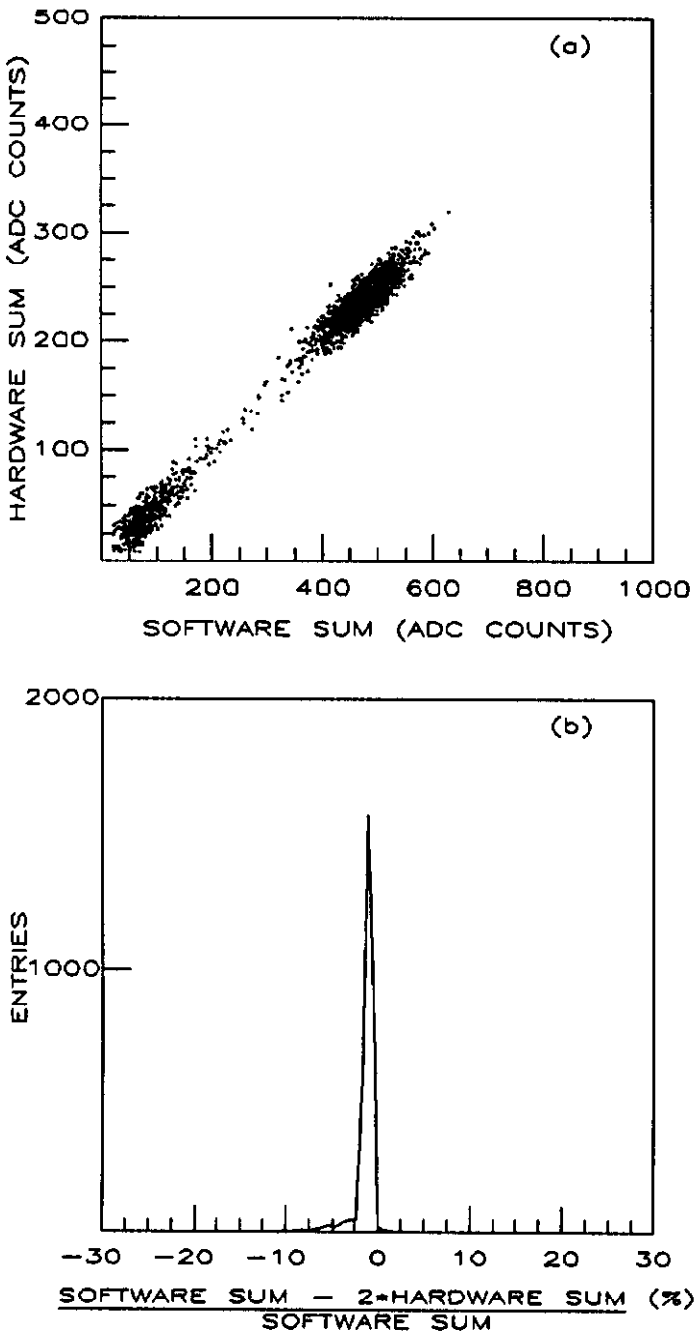

Fig. 9. Hardware sum vs. reconstructed software sum (a) and the percentage difference between the hardware and software sums (b) for the level I summer. The hardware sum is attenuated by a a factor of 2 relative to the software sum. The data were taken at an electron beam at BNL.

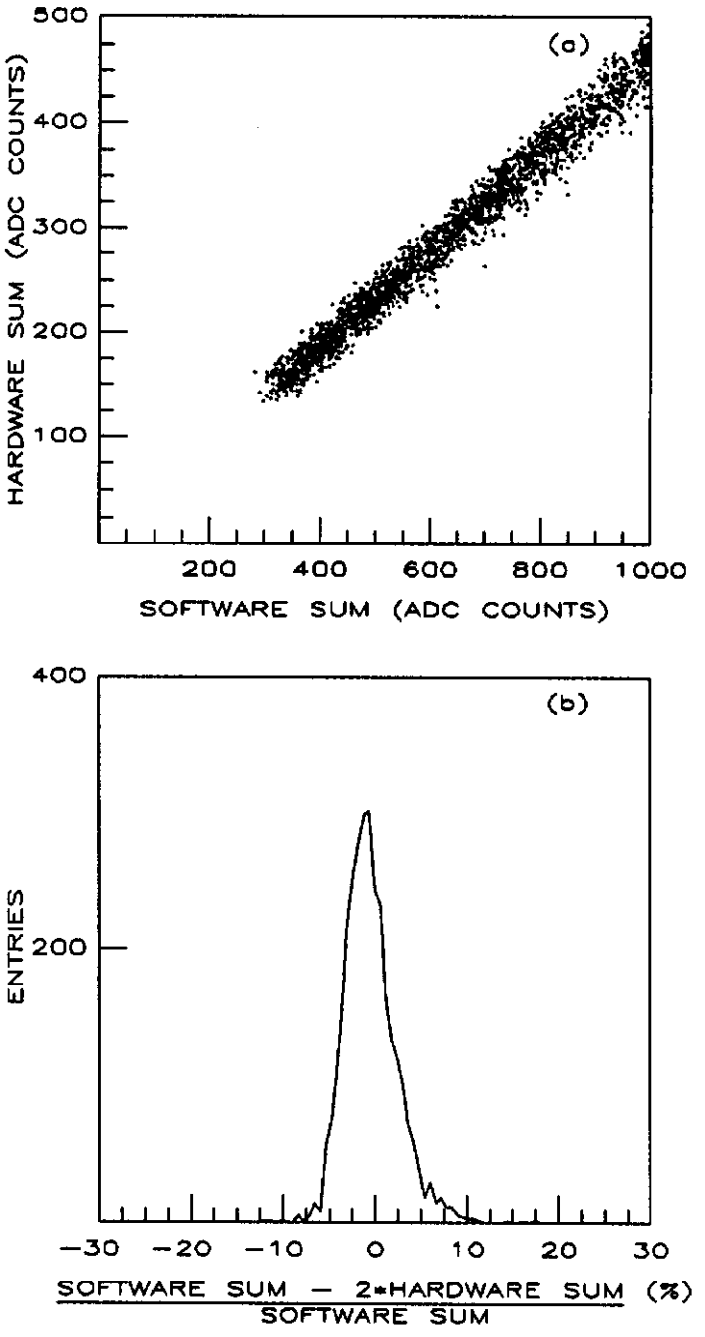

Fig. 10. Hardware sum vs. reconstructed software sum (a) and the percentage difference between the hardware and software sums (b) for the 40 super-clusters from the level II summers. These data were taken during the 1990 E760 run while scanning the ψ' resonance.

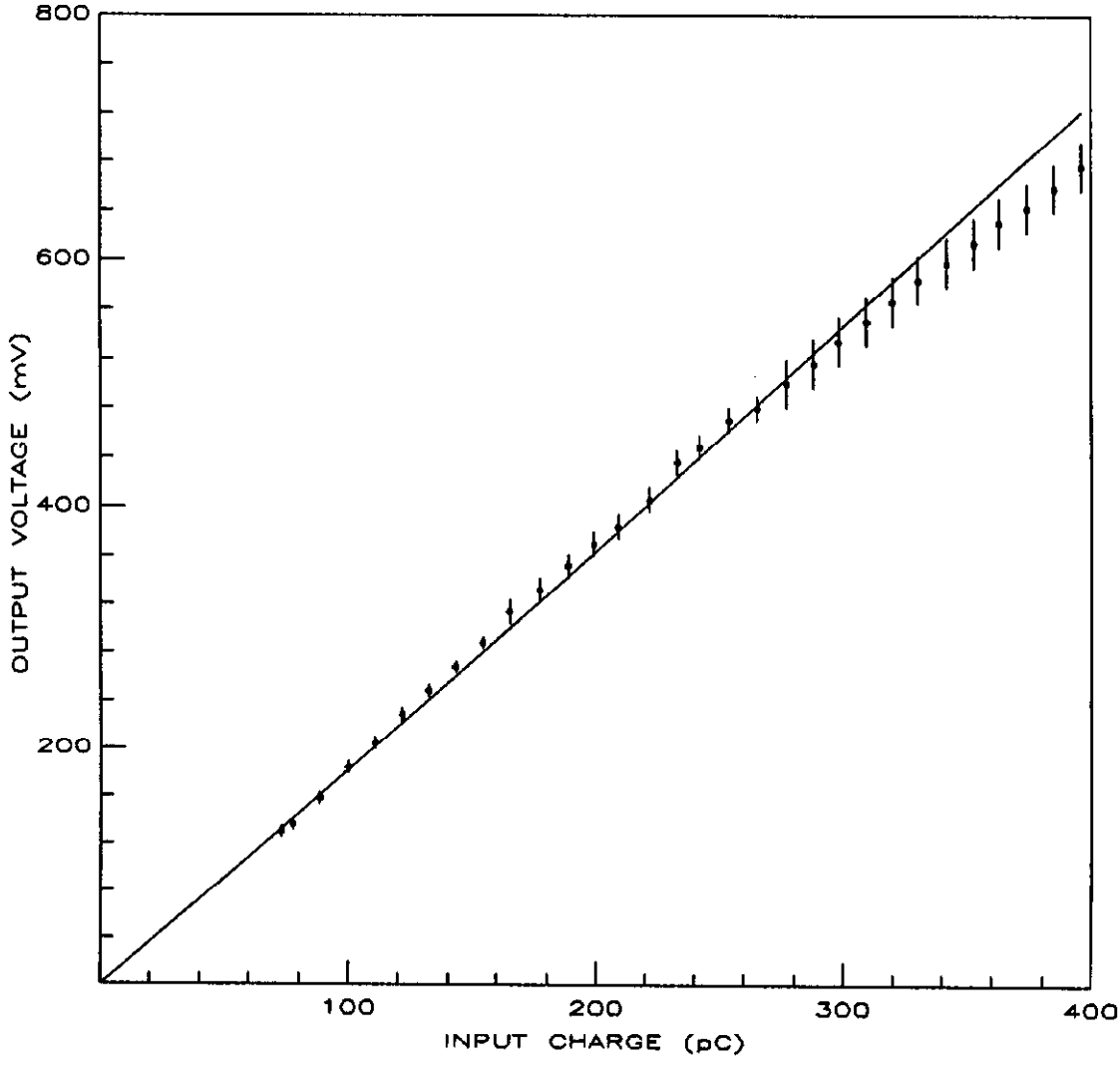

Fig. 11. Linearity plot of output voltage vs. input charge for the integrator circuit. The straight line fit has a χ^2/d.o.f. of 1.3. The largest thresholds set are in the 200 pC range.

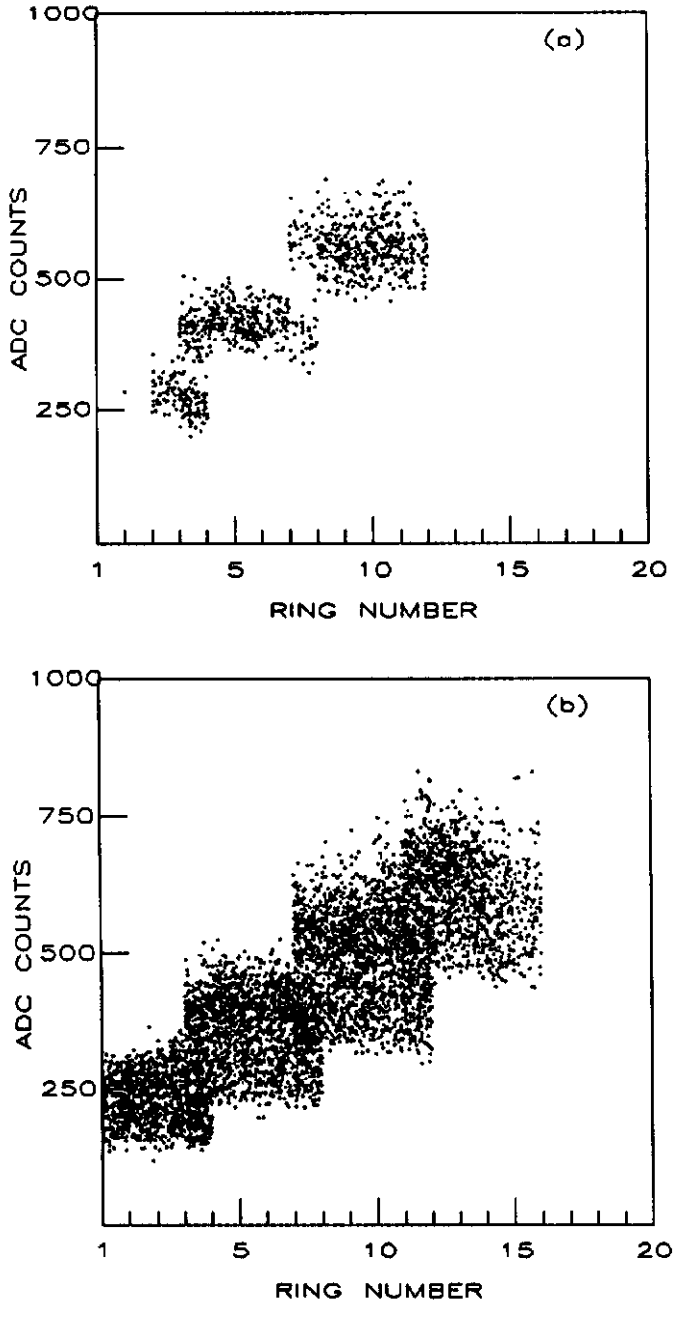

Fig. 12. Hardware sum from the level II summers vs. ring number for both tracks of reconstructed ψ's (a) and for the case when any sum has its corresponding pattern unit bit set (b). The bottom edge of the distributions in (b) indicate the energy threshold levels. These data were taken during the 1990 E760 run at the ψ resonance.